Journal of Alloys and Compounds 507 (2010) 157–161

Contents lists available at ScienceDirect

Journal of Alloys and Compounds

journal homepage: www.elsevier.com/locate/jallcom

Effect of Eu substitution on the crystal structure and multiferroic properties of $BiFeO_3$

Xingquan Zhang[a], Yu Sui[a,b,*], Xianjie Wang[a], Yang Wang[c], Zhu Wang[a]

[a] Center for Condensed Matter Science and Technology (CCMST), Department of Physics, Harbin Institute of Technology, Harbin 150001, PR China
[b] International Centre for Materials Physics, Chinese Academy of Sciences, Shenyang 110016, PR China
[c] Division of Physics and Applied Physics, School of Physical and Mathematical Sciences, Nanyang Technological University, 21 Nanyang Link, 637371 Singapore

ARTICLE INFO

Article history:
Received 13 April 2010
Received in revised form 19 July 2010
Accepted 20 July 2010
Available online 29 July 2010

Keywords:
Multiferroic
$BiFeO_3$
Substitution
Magnetoelectric coupling

ABSTRACT

Single-phase $Bi_{1-x}Eu_xFeO_3$ ($0 \le x \le 0.3$) multiferroic ceramics were prepared to study the effects of Eu substitution on their crystal structure and ferroelectromagnetic behavior. X-ray diffraction studies revealed a sequence of the composition-driven structural phase transitions R3c → $Pn2_1a$ (occurs at $x = 0.2$). Magnetic measurements revealed that Eu substitution can effectively induce the appearance of the spontaneous magnetization, which was significantly enhanced upon the composition-driven transition from a rhombohedral to an orthorhombic phase. The leakage current was found to be reduced on increased Eu concentration. The electric hysteresis loops were obtained in the $Bi_{1-x}Eu_xFeO_3$ ceramics, but the loops were not really saturated. The magnetoelectric coupling in Eu-doped $BiFeO_3$ was estimated by the changes in the dielectric constant with an external magnetic filed.

1. Introduction

Multiferroic materials exhibiting coexistence and simultaneous coupling of ferroelectricity and ferromagnetism have recently attracted considerable attention due to their potential applications and attractive physical phenomena [1–3]. As one of representative single-phase multiferroics, $BiFeO_3$ (BFO) is known to be the only material that is both ferroelectric ($T_C \sim 1103$ K) and antiferromagnetic ($T_N \sim 643$ K) at room temperature, which makes it an excellent possible candidate for practical application [4]. However, it is difficult to obtain a good polarization hysteresis (P–E) loop and a large remnant polarization (P_r) in BFO, especially in the BFO ceramics, due to the high leakage current and low resistance caused by defects such as secondary phases and oxygen vacancies [5,6]. Furthermore, BFO has a spiral spin structure with an incommensurate spiral period of ~62 nm, which superimposes on the antiferromagnetic ordering and results in the cancellation of net magnetization [7].

Several research groups have tried *A*-site (Bi-site) substituting by using rare-earth ions (RE) to modify the multiferroic properties of BFO in recent years [8–19]. Low-level substitutions of rare-earth ions for bismuth have some interesting effects: (i) partial substitutions of rare-earth ions (e.g., La^{3+}, Pr^{3+}, or Sm^{3+}) for bismuth help in eliminating the secondary phase along with a structural phase transition improving ferroelectric properties of BFO. (ii) The introduction of rare-earth cations in BFO seems to increase the magnetocrystalline anisotropy, thus making the cycloidal spin structure energetically unfavorable. Nalwa et al. [8] have reported that Sm doping can enhance the formation of perovskitic Sm-doped BFO phase and eliminate the impurity phase formation. Singh et al. [9] and Kazhugasalamoorthy et al. [10] suggested that La^{3+} substitution for Bi^{3+} eliminates impurity phases along with a structural phase transition improving ferroelectric properties and also help in improving the magnetic properties. Kazhugasalamoorthy et al. [10] also reported that, for 20% and 30% La modification, the structure of BFO changes from rhombohedral to the orthorhombic and tetragonal respectively. Liu et al. [11], in their investigations of Ce-doped BFO thin films, reported a change in the crystal structure of the material which resulted in improved the ferroelectric, fatigue and magnetic properties. Furthermore, measurements of the dielectric constant as a function of magnetic field revealed the presence of a linear magnetoelectric effect for $Bi_{0.85}La_{0.15}FeO_3$ [14], $Bi_{0.8}Pr_{0.2}FeO_3$ [15] and $Bi_{0.8}Dy_{0.2}FeO_3$ [16], which was chosen as representative, thus providing evidence of the possibility of substitution-induced spin cycloid suppression. Moreover, direct evidence of cycloid suppression in BFO was given via nuclear magnetic resonance measurements on La-substituted samples, which showed that the modulated structure disappears at $x = 0.2$, and its destruction is correlated with the structural transition from the rhombohedral (R3c) to an orthorhombic (C222) cell [17]. Later

* Corresponding author at: Center for Condensed Matter Science and Technology (CCMST), Department of Physics, Harbin Institute of Technology, P.O. Box 3025, Science Park, Harbin 150001, PR China. Tel.: +86 451 86418403; fax: +86 451 86418403.
E-mail address: suiyu@hit.edu.cn (Y. Sui).

0925-8388/$ – see front matter © 2010 Elsevier B.V. All rights reserved.
doi:10.1016/j.jallcom.2010.07.144

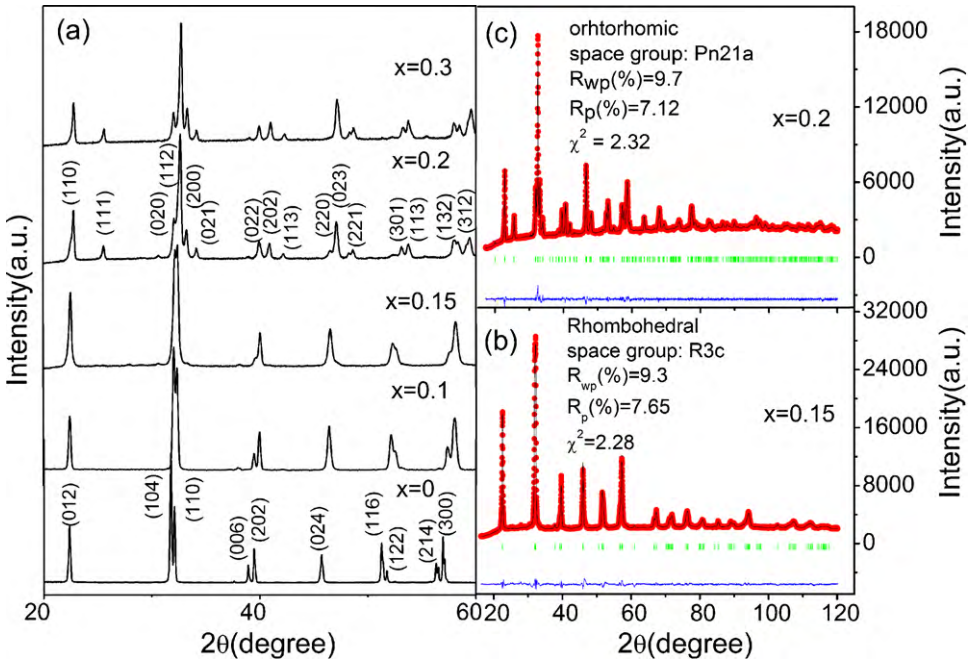

Fig. 1. (a) XRD patterns of the $Bi_{1-x}Eu_xFeO_3$ ceramics. (b and c) Observed (solid circles), calculated (solid line), and difference (solid line at the bottom) XRD patterns for $Bi_{0.85}Eu_{0.15}FeO_3$ (R3c mode) and $Bi_{0.8}Eu_{0.2}FeO_3$ ($Pn2_1a$ model) at room temperature. Bragg reflections are indicated by ticks.

investigations revealed that there is a strong dependence of the magnetic response with the size of the dopant ion responsible of the cycloidal coupling of spins suppression in BFO [18]. It was found that the most effective way to induce spontaneous magnetization in BFO should be related to the substitution with ions, possessing a large difference in ionic radius with respect to that of Bi^{3+}. Indeed, for RE = Gd and Dy [19,20], which has the smaller ionic radius, 15% doping is sufficient to induce a structure transition and spontaneous magnetization in these systems.

Although several experiments were performed on $Bi_{1-x}RE_xFeO_3$ multiferroic compounds in recent years, minor attention has been paid to Eu-substituted BFO [21–25]. Compared with Bi^{3+} ion (radius = 1.17 Å), Eu^{3+} ion (1.07 Å) possesses a much smaller radius [26], which indicates that substitution of Eu^{3+} for Bi^{3+} in BFO would cause a more significant structural distortion and suppress of spin cycloid in BFO effectively and therefore improve the magnetic properties of BFO. However, existing papers focus on certain physical characteristics of some Eu-containing samples and do not give a clear understanding of what is going on with the crystal structure, ferroelectric and magnetic properties of the solid solutions upon Eu substitution. Moreover, the reported phase relations of the system are not consistent with each other. A solution limitation was found near 10% mol for Eu-doped BFO nanoparticles [21], however, Troyanchuk et al. [22] reported a transition of rhombohedral (R3c) to orthorhombic (Pnma) for 20% mol doping percentage of Eu in BFO. A structural transformation from rhombohedral to triclinic has also been revealed in this system by Reddy et al. [23]. In the present work, we prepared single-phase multiferroic of Eu-substituted $Bi_{1-x}Eu_xFeO_3$ ($x = 0$, 0.1, 0.15, 0.2, and 0.3) samples and investigated the influence of the Eu substitution on the crystal structure, and multiferroic properties of BFO ceramic systematically.

2. Experimental

Polycrystalline $Bi_{1-x}Eu_xFeO_3$ ($x = 0$, 0.1, 0.15, 0.2, and 0.3) samples were prepared by the rapid liquid phase sintering method [27]. High purity powders of Bi_2O_3, Eu_2O_3, and Fe_2O_3 were used as starting materials. After weighing and ball milling, the mixed powders were dry pressed into small discs with a diameter of ~8 mm and thickness of ~1 mm. The discs were dehydrated at 150 °C for 12 h in a vacuum chamber before being sintered at a relatively high temperature for a short time of 20 min. The optimized synthesized temperatures were 850 °C, 850 °C, 865 °C, 865 °C and 870 °C for $x = 0$, 0.1, 0.15, 0.2 and 0.3, respectively. Crystallographic structure analysis was performed by X-ray diffraction (XRD) using a Bede D^1 XRD diffractometer with Ni filtered Cu K_α ($\lambda = 0.15406$ nm) radiation. XRD data were collected at slow scan with a 2θ step size of 0.02° and at a scan rate of one step every 6 s. Simulation of crystal structure based on the measured XRD data was performed using a Rietveld crystal structure refinement software (FULLPROF 2000). The ferroelectric hysteresis loops and leakage currents of the samples were measured using a Precision Premier Workstation (Radiant Technology, USA). For the measurements of electrical properties, the disks (6 mm diameter, 0.4–0.5 mm thick) were carefully polished and Ag electrodes were applied on both surfaces to form metal-insulator-metal capacitors. The polarization hysteresis (P–E) loops were acquired at a frequency of 100 Hz. Dielectric measurements were carried out in the frequency range (100 Hz–1 MHz) using an impedance analyzer (HP 4194 A). Magnetic properties of the samples were obtained using the physical properties measurement system (PPMS) of Quantum Design. Magnetization curves were obtained at 300 K in an applied magnetic field range of $\pm 3.98 \times 10^6$ A/m.

3. Results and discussion

Fig. 1(a) shows the XRD patterns of $Bi_{1-x}Eu_xFeO_3$ samples. It can be seen that all the samples exhibit single-phase characteristics with no trace of other impurity phases (e.g., Eu_2O_3, $Bi_2Fe_4O_9$, etc.) The diffraction peaks in the patterns of $x \leq 0.15$ samples characterize a polycrystalline rhombohedrally distorted perovskite structure, and the doubly split peaks of BFO overlap partially to form a broadened peak in the 2θ ranges of 38–40° and 51–53° with increasing the Eu concentration. For the compounds with $0.2 \leq x \leq 0.3$, it is obvious that the XRD patterns are close to that of orthorhombic $EuFeO_3$ [28], suggesting a structural phase transition at $x = 0.2$. In order to further analyze such transformation, the measured XRD patterns of $Bi_{1-x}Eu_xFeO_3$ samples were analyzed with Rietveld refinement program. The best fits to the measured data are observed using rhombohedral lattice type with R3c space group for $x \leq 0.15$ samples and with orthorhombic lattice type with $Pn2_1a$ space group for $x \geq 0.2$ samples. The typical fitted results of $Bi_{0.85}Eu_{0.15}FeO_3$ and $Bi_{0.8}Eu_{0.2}FeO_3$ are shown in Fig. 1(b) and (c), respectively, in which the simulated XRD patterns agree well with the measured XRD patterns. The crystal structure parameters derived from the Rietveld refinement program are listed in

Table 1
The crystal symmetry and unit cell parameters of the $Bi_{1-x}Eu_xFeO_3$ samples obtained by Rietveld refinement of the XRD patterns.

Sample	Space group	a (Å)	b (Å)	c (Å)	Volume (Å^3 per primitive cell)
$BiFeO_3$	R3c	5.5797	5.5797	13.8593	368.24
$Bi_{0.9}Eu_{0.1}FeO_3$	R3c	5.5712	5.5712	13.8194	367.78
$Bi_{0.85}Eu_{0.15}FeO_3$	R3c	5.5624	5.5624	13.7593	366.62
$Bi_{0.8}Eu_{0.2}FeO_3$	*Pn*21*a*	5.6223	7.7788	5.4195	238.14
$Bi_{0.7}Eu_{0.3}FeO_3$	*Pn*21*a*	5.6331	7.7949	5.4277	238.92

Table 1. Taking into account that the $Pn2_1a$ space group is non-centrosymmetric and allows polar ionic displacements along the (010) direction [19], we can conclude that Eu substitution induce a polar-to-polar R3c → $Pn2_1a$ structural phase transition at $x = 0.2$ in $Bi_{1-x}Eu_xFeO_3$ compounds. Therefore, coexistence of ferroelectric polarization and net magnetization can be expected within these compounds. The structure transformation from rhombohedral phase (R3c) to orthorhombic phase ($Pn2_1a$) induced by Eu substitution can be attributed to the size effect. It is known that the ferroelectric distortion of BFO is mainly caused by the hybridization of Bi 6s and O 2s/2p orbitals. The R3c structure of BFO can be regarded as evolving from the ideal cubic perovskite structure Pm3m with two types of distortions. One is the ferroelectric distortion along the [1 1 1] axis of the cubic perovskite structure, resulting in Pm3m → R3m. The other is a relative rotation of two oxygen octahedra in the opposite direction around [1 1 1], resulting in Pm3m → R3c. Compared with Bi^{3+} ion (radius = 1.17 Å), Eu^{3+} ion (1.07 Å) possesses a much smaller radius. As the smaller, less polarizable Eu^{3+} substitutes for Bi^{3+} ions, the tolerance factor (t) decrease:

$$t = \frac{R_A + R_O}{\sqrt{2}(R_B + R_O)};$$

where R_A, R_B, and R_O are the ionic radii of the A, B, and O sites. When the tolerance factor is smaller than unity, the Fe–O bonds are under compression and the Bi^{3+}/Eu^{3+}–O bonds are under tension. The oxygen octahedra then tend to rotate cooperatively to alleviate the lattice stress [29] and the relative rotation angle of the two oxygen octahedra around the polarization [1 1 1] axis in the R3c unit cell for the samples increases with substitution of Eu for Bi in BFO. As Eu concentration increases, the induced distortions make the rhombohedral phase unstable and consequently stabilize the orthorhombic phase, shrinking lattice parameters as well as the overall volume of the unit cell.

Fig. 2(a) shows the room temperature P–E hysteresis loops of $Bi_{1-x}Eu_xFeO_3$ ceramics. For pure BFO sample, a very weak polarization of 0.2 μC/cm^2 was observed under an applied field of 10 kV/cm. Although all the Eu-doped samples exhibited improved polarization, the P–E loops of the Eu-doped BFO samples do not show saturated hysteresis loops as obtained previously in the epitaxial films [30] and single crystals [31]. The contributions to the apparent ferroelectric loop possibly arise from the leakage contributions.

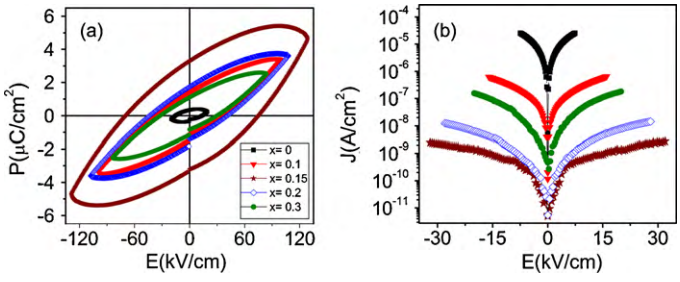

Fig. 2. (a) Ferroelectric hysteresis (P–E) loops for $Bi_{1-x}Eu_xFeO_3$ ceramics at room temperature. (b) Leakage current as a function of applied electrical field in $Bi_{1-x}Eu_xFeO_3$ ceramics.

Previous studies on polycrystalline BFO ceramics have shown similar ferroelectric hysteresis loops [32,33] as in the present work. In the presence of conducting phases, to suppress the leakage and thus to extract the intrinsic ferroelectric behavior of BFO, low temperature measurements will be needed. To get more insight into the electrical properties, we carried out the leakage measurements on these samples which are shown in Fig. 2(b). For the case of BFO ceramic, the leakage current increases as the electric field increases before it breaks down at about 7 kV/cm. The relatively higher leakage of BFO is known to be attributed to the presence of charged oxygen vacancies, compensating electronic charge carriers, mixed valences of Fe (Fe^{2+} and Fe^{3+}). Moreover, large grain boundary area coupled with higher space charge density is also likely to result in higher leakage in BFO ceramics [34,35]. Previous works [30] revealed that doping of lanthanides can suppress the formation of oxygen vacancies in BFO ceramics and films, suppressing the leakage current of BFO. Indeed, doping of Eu can reduce the leakage current of BFO and the leakage current density of the Eu-doped ceramics is lowered two to four orders of magnitude in comparison with pure BFO ceramics. However, although the leakage current density is reduced still it was not possible to apply high electric fields for Eu-substituted BFO samples at room temperature. It can also be found that the leakage current does not decrease monotonically with the increase of the Eu content, which could be attributed to the reason that the microstructure of $Bi_{0.8}Eu_{0.2}FeO_3$ and $Bi_{0.7}Eu_{0.3}FeO_3$ ceramics is not as homogeneous as that of $Bi_{0.9}Eu_{0.1}FeO_3$ ceramic. To conclusively understand the role of defects in conduction in BFO, comprehensive impedance spectroscopy studies are needed to investigate these issues and will be part of further work.

BFO is known to be antiferromagnetic with a G-type magnetic structure. Since the spin order in BFO ceramic is spatially modulated, it has no macroscopic magnetization at room temperature [7]. The magnetization hysteresis (M–H) loops of $Bi_{1-x}Eu_xFeO_3$ samples are shown in Fig. 3. It is evident that the antiferromagnetic nature in BFO evolves into weak ferromagnetism with a small remnant magnetization (M_r) in Eu-doped BFO samples. The mea-

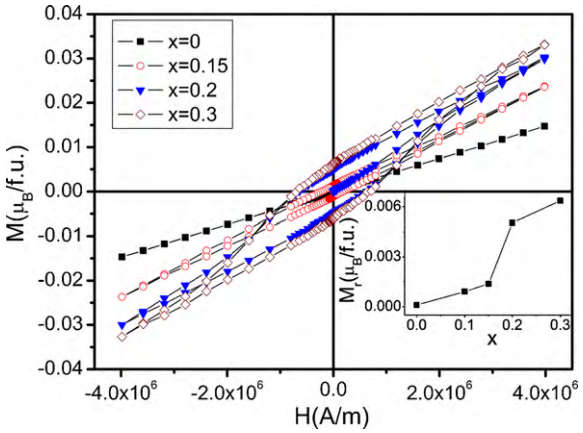

Fig. 3. Field dependences of the magnetization obtained for $Bi_{1-x}Eu_xFeO_3$ ($x = 0$, 0.15, 0.2 and 0.3) samples at room temperature.

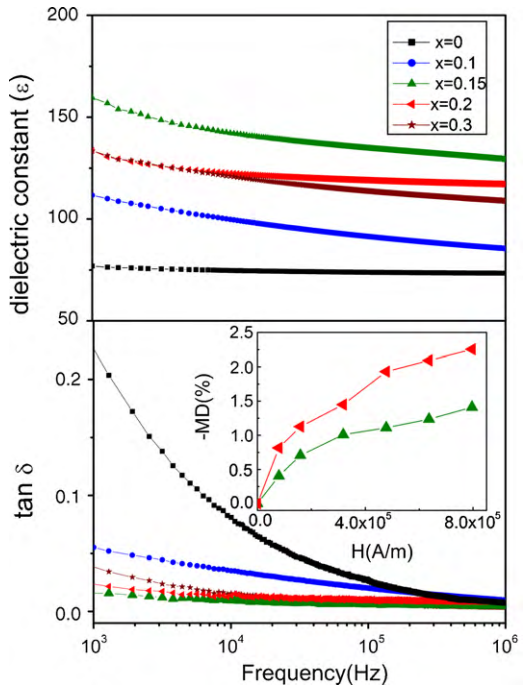

Fig. 4. (a) Frequency dependence of the dielectric constant for the $Bi_{1-x}Eu_xFeO_3$ samples at room temperature; (b) Frequency dependence of the dielectric loss for the $Bi_{1-x}Eu_xFeO_3$ samples at room temperature. The inset shows the magnetic field-induced change in dielectric constant of $Bi_{0.85}Eu_{0.15}FeO_3$ and $Bi_{0.8}Eu_{0.2}FeO_3$ measured at room temperature.

sured M_r values as a function of x were also shown in the inset of Fig. 3. A step-like increase in M_r is observed and the M_r values of $Bi_{1-x}Eu_xFeO_3$ with $x \leq 0.15$ are significantly less than that of $Bi_{0.8}Eu_{0.2}FeO_3$. These results are in accordance with the change in the crystal structure caused by Eu doping and indicate the weak ferromagnetism obtained in $Bi_{1-x}Eu_xFeO_3$ should be related to an antisymmetric exchange mechanism [36], and the substitution-induced suppression of the spiral spin modulation should be its prime cause [18,37]. For the Eu-doped BFO samples, when $x \leq 0.15$, the Eu substitution can only suppress but cannot destruct the spin cycloid, leading to limited increase of M_r value. However, when $x \geq 0.20$, the Eu substitution results in structural phase transition wherein the spin cycloid might be destructed and homogeneous spin structure formed, so that the latent magnetization locked within the cycloid might be released and significant increased M_r value is observed.

Fig. 4(a) and (b) illustrates the frequency (f) dependences of relative dielectric constant ε and dielectric loss ($\tan\delta$) for the $Bi_{1-x}Eu_xFeO_3$ samples. All samples display a decreasing trend in ε and $\tan\delta$ with increasing f from 1000 Hz to 1 MHz. The observation has been explained by the phenomenon of dipole relaxation wherein at low frequencies the dipoles are able to follow the frequency of the applied field. Eu-doped BFO possesses a larger ε from 75 for pure BFO to 158 for $Bi_{0.85}Eu_{0.15}FeO_3$ at 3 kHz. To examine possible magnetoelectric coupling in $Bi_{1-x}Eu_xFeO_3$, we investigated the magnetic field dependence of dielectric constant. The variation of the dielectric constant as a function of the magnetic field was defined as the following formula:

$$\mathrm{MD} = \frac{\varepsilon(H) - \varepsilon(0)}{\varepsilon(0)} \quad (1)$$

where MD (%) is magnetodielectric coefficient, $\varepsilon(H)$ and $\varepsilon(0)$ are the dielectric constants at applied magnetic field and zero field, respectively. The room temperature values of MD for $Bi_{0.85}Eu_{0.15}FeO_3$ and $Bi_{0.8}Eu_{0.2}FeO_3$ measured at 3 kHz under varying magnetic fields are shown in the inset of Fig. 4(b). The dielectric constant decreases with increasing field; the values of MD effect are −1.4% and −2.2% for $Bi_{0.85}Eu_{0.15}FeO_3$ and $Bi_{0.8}Eu_{0.2}FeO_3$ at $\Delta H = 7.96 \times 10^5$ A/m, respectively. Similar phenomena were also observed in Dy doped BFO [16]. Palkar et al. pointed out that such behavior originates from the coupling between the magnetic and ferroelectric domain [38]. In multiferroics, when a magnetic field is applied, the materials will be strained. Due to the coupling between the magnetic and ferroelectric domain, the strain will induce stress and then generate an electric field on the ferroelectric domain. As a result, the dielectric behavior will be modified.

4. Conclusions

In conclusion, single-phase $Bi_{1-x}Eu_xFeO_3$ ceramics with varying x from 0 to 0.3 were prepared by rapid liquid phase sintering method. We have studied the influence of Eu doping on the crystal structure, the magnetic and ferroelectric behavior of the BFO. X-ray diffraction studies revealed phase transition from rhombohedral (R3c) to orthorhombic ($Pn2_1a$) at substitution of 20% mol of Eu. It was found that the phase transition destructs the spin cycloid of BFO, and therefore, releases the locked magnetization and results in significantly improved magnetic properties. It was also found that the doping of Eu can effectively reduce the leakage current density of BFO and improve the ferroelectric properties. The change in the dielectric constant with applied magnetic field suggests that magnetoelectric coupling exists in these compounds.

Acknowledgements

This work is supported by the National Natural Science Foundation of China (Grant Nos. 50672019 and 10804024). The project was sponsored by the Scientific Research Foundation for the Returned Overseas Chinese Scholars, State Education Ministry. The project (HIT. NSRIF.2009056) was supported by the natural scientific research innovation foundation in Harbin Institute of Technology.

References

[1] M. Fiebig, J. Phys. D 38 (2005) R123.
[2] K.F. Wang, J.M. Liu, Z.F. Ren, Adv. Phys. 58 (2009) 321.
[3] C.W. Nan, M.I. Bichurin, S.X. Dong, D. Viehland, G. Srinivasan, J. Appl. Phys. 103 (2008) 031101.
[4] J. Wang, J.B. Neaton, H. Zheng, V. Nagarajan, S.B. Ogale, B. Liu, D. Viehland, V. Vaithyanathan, D.G. Schlom, U.V. Waghmare, N.A. Spaldin, K.M. Rabe, M. Wuttig, R. Ramesh, Science 299 (2003) 1719.
[5] G. Catalan, J.F. Scott, Adv. Mater. 21 (2009) 321.
[6] X.D. Qi, J. Dho, R. Tomov, M.G. Blamire, J.L. MacManus-Driscoll, Appl. Phys. Lett. 86 (2005) 062903.
[7] C. Ederer, N.A. Spaldin, Phys. Rev. B 71 (2005) 224103.
[8] K.S. Nalwa, A. Garg, J. Appl. Phys. 103 (2008) 044101.
[9] A. Singh, A. Gupta, R. Chatterjeea, Appl. Phys. Lett. 92 (2008) 152905.
[10] S. Kazhugasalamoorthy, P. Jegatheesan, R. Mohandoss, B. Karthkeran, R.J. Joseyphus, S. Dhanuskodi, J. Alloys Compd. 493 (2010) 569.
[11] J. Liu, M.Y. Li, L. Pei, J. Wang, B.F. Yu, X. Wang, X.Z. Zhao, J. Alloys Compd. 493 (2010) 544.
[12] N. Kumar, N. Panwar, B. Gahtori, N. Singh, H. Kishan, V.P.S. Awana, J. Alloys Compd. 501 (2010) L29.
[13] X.H. Zheng, Q.Y. Xu, Z. Wen, X.Z. Lang, D. Wu, T. Qiu, M.X. Xu, J. Alloys Compd. 499 (2010) 108.
[14] G. Le Bras, D. Colson, A. Forget, N. Genand-Riondet, R. Tourbot, P. Bonville, Phys. Rev. B 80 (2009) 134417.
[15] P. Uniyal, K.L. Yadav, J. Phys.: Condens. Matter. 21 (2007) 405901.
[16] F.Z. Qian, J.S. Jiang, S.Z. Guo, D.M. Jiang, W.G. Zhang, J. Appl. Phys. 106 (2009) 084312.
[17] A.V. Zalesskii, A.A. Frolov, T.A. Khimich, A.A. Bush, Phys. Solid State 45 (2003) 141.
[18] J. Andrés, M. Cagigas, D.S. Candela, E. Baggio-Saitovitch, J. Phys.: Conf. Ser. 200 (2010) 012134.
[19] V.A. Khomchenko, D.A. Kiselev, I.K. Bdikin, V.V. Shvartsman, P. Borisov, W. Kleemann, J.M. Vieira, A.L. Kholkin, Appl. Phys. Lett. 93 (2008) 262905.
[20] S.X. Zhang, W.J. Luo, L. Wang, D.L. Wang, Y.W. Ma, J. Appl. Phys. 107 (2010) 054110.
[21] J. Liu, L. Fang, F.G. Zheng, S. Ju, M.R. Shen, Appl. Phys. Lett. 95 (2009) 022501.

[22] I.O. Troyanchuk, M.V. Bushinsky, D.V. Karpinsky, O.S. Mantytskaya, V.V. Fedotova, O.I. Prochnenko, Phys. Status Solidi B (2009) 1–7.
[23] V.R. Reddy, D. Kothari, A. Gupta, S.M. Gupta, Appl. Phys. Lett. 94 (2009) 082505.
[24] P. Uniyal, K.L. Yadav, J. Appl. Phys. 105 (2009), 07D914.
[25] V.F. Freitas, H.L.C. Grande, S.N. de Medeiros, I.A. Santos, L.F. Cotica, A.A. Coelho, J. Alloys Compd. 461 (2008) 48.
[26] R.D. Shannon, Acta Crystallogr. A32 (1976) 751.
[27] Y.P. Wang, L. Zhou, M.F. Zhang, X.Y. Chen, J.M. Liu, Z.G. Liu, Appl. Phys. Lett. 84 (2004) 1731.
[28] S.Z. Li, Y.J. Huang, J.B. Zhu, Y. Zhang, N. Chen, Y.F. Hsia, Phys. B: Condens. Matter. 393 (2007) 100.
[29] J.B. Li, G.H. Rao, Y. Xiao, J.K. Liang, J. Luo, G.Y. Liu, J.R. Chen, Acta Mater. 58 (2010) 3701.
[30] G.D. Hu, X. Cheng, W.B. Wu, C.H. Yang, Appl. Phys. Lett. 91 (2007) 232909.
[31] D. Lebeugle, D. Colson, A. Forget, M. Viret, Appl. Phys. Lett. 91 (2007) 022907.
[32] D. Maurya, H. Thota, K. Singh Nalwa, A. Garg, J. Alloys Compd. 477 (2009) 780.
[33] D.H. Wang, W.C. Goh, M. Ning, C.K. Ong, Appl. Phys. Lett. 88 (2006) 212907.
[34] R. Schmidt, W. Eerenstein, T. Winiechi, F.D. Morrison, P.A. midgley, Phys. Rev. B 75 (2007) 24511.
[35] A. Srivastava, A. Garg, F.D. Morrison, J. Appl. Phys. 105 (2009) 054103.
[36] T. Moriya, Phys. Rev. 120 (1960) 91.
[37] A.M. Kadomtseva, Y.F. Popov, A.P. Pyatakov, G.P. Vorob'ev, A.K. Zvezdin, D. Viehland, Phase Transit. 79 (2006) 1019.
[38] V.R. Palkar, D.C. Kundaliya, S.K. Malik, S. Bhattacharya, Phys. Rev. B 69 (2004) 212102.